Wasit Journal of Engineering Sciences
Journal homepage: https://ejuow.uowasit.edu.iq
ISSN 2305-6932
Original Research
Vol. 14 No. 2 June 2026, pp.320-337
https://doi.org/10.31185/ejuow.v14i2.875

Evaluating Hybrid Heat Sink Designs Incorporating Metal Foam, Phase Change Materials, and Air Channels

Maryam Alathraa Saad[1], Abbas J. Jubear Al- jassani[1], Mohammed G. Muhssen[1], Adel G Nasser[2]
[1]Wasit University, College of Engineering, Mechanical Engineering Department, Al-kut-Wasit 52001, Iraq|
[2]Department of Fluid and Environment, School of Engineering, Faculty of Science and Engineering, University of Manchester, UK

Corresponding Author Email: abbasaljassani@uowasit.edu.iq

Received Oct.22, 2025 Revised Feb.17, 2026 Accepted Feb.19, 2026 Online Jun.1, 2026

Abstract

This paper provides an extensive comparative study of the thermal management performance of hybrid heat sink systems using phase change materials (PCMs) and air subjected to different levels of heat flux from 2500 - 10000 W/m². Five different configurations were tested: air, foam/air, paraffin/air, organic material OM air, and finned heat sink HS wax hybrids. It was determined from the data collected that the air-only, baseline system is inadequate for high-thermal-load conditions (i.e., 840 K maximum base temperature), while PCM-based heat sink systems were able to function effectively in preventing thermal saturation via the establishment of an isothermal plateau condition. The results performed with low heat flux (2500 W/m²) OM and HS wax configurations created a base temperature of 325 K that lasted for approximately 50 minutes providing us with the opportunity to operate 5 times longer than with air only. Thermal Enhancement Ratio (TER) analysis indicated that OM wax was able to achieve a maximum TER of 3.0 at 60°C while paraffin wax was maximum at the threshold of 80°C with a TER of 2.3 under 5000 W/m². The HS-wax hybrid achieved an approximate liquid fraction of 1.0 in about 4–6 min given that it has better conductivity due to the enhanced metallic fins and therefore provided better thermal uniformity than the others. With the extreme load (10000 W/m²), the performance of all PCMs converged and the value of the TER dropped down to approximately 2.0 and the operational times were only 13–15 min for a 100°C target. In conclusion, although PCMs significantly reduce peak temperatures decrease 840 K to 590 K at 10000 W/m², latent heat capacity remains the limiting factor under conditions of high thermal loads high intensities when thermally breaking through.

Keywords: PCM, Heat Sink, Paraffin Wax, Latent Heat, Thermal Overshoot, Numerical Study, Transient Analysis, Foam.

1. Introduction

As the miniaturization of power electronics continues, extreme heat flux densities become increasingly difficult to handle with existing methods of cooling. Traditional methods, such as air-cooled heat sinks, have difficulty maintaining junction temperature limits during transient peak loads, since air does not have very high thermal conductivity or heat capacity. Therefore, there is a need to create hybrid cooling systems that include both active convective cooling and passive thermal storage for reliable operation[1], [2]. Phase chang materials (PCMs) are a good source of transient cooling as they can store large quantities of energy in the form of latent heat. However, low thermal conductivity is the main factor limiting the performance of PCM due to the amount of heat that can penetrate [3], [4]. Open-cell metallic foams provide an alternative that promotes convective heat transfer by maximizing the surface area relative to volume and creating turbulence in the flow of air. There is, however, very limited data available in the literature for a "sectional hybrid" design, defined as a design in which air channels are strategically alternated with functional materials to provide the best balance between thermal performance and weight [6].

Researchers have assessed the role of metal foam attributes in terms of how well they can facilitate the use of phase change material (PCM) as a heat storage medium in conjunction with metal foams acting as heat sinks [7]. Based on experimental data and artificial neural networks (ANNs), Duan and Li [8] determined that

porosity is the most significant factor affecting both the melting rate of PCM and the corresponding amount of heat flow from the metal to the PCM. In addition, Chen et al. [9] conducted tests with hybrid active cooling systems that included both micro-encapsulated phase change material and slurry nano-particles within microchannels. Results from these experiments showed that the addition of micro-encapsulated and/or nanoparticle slurries led to a significant increase in the Nusselt number and a decrease in the wall temperature. However, they also warned that high concentrations of either of the two added materials would significantly increase the resistance to the flow of coolant. A study conducted by Stever et al. [10] included the enhancement of thermal conductivity by sodium acetate trihydrate (SAT) being infused into copper foams coated with disodium hydrogen phosphate dodecahydrate. The resulting thermal conductivity of 2.62 W/m K for the 80 PPI foam matrix (approximately four times as much as SAT alone) was particularly noted due to its ability to reduce or completely eliminate the effects of supercooling. Another study performed by Mirshekar et al. [11] demonstrated that the combination of paraffin RT55 embedded into copper foams accelerates the heating and cooling cycles as compared to bare copper foams, as well as improving temperature distribution overall. Taken together, the results of these studies demonstrate that although metal foam structures provide an optimal thermal conductivity and thermal response, there are trade-offs in terms of porosity and flow resistance between these two criteria.

Computational modelling research has further developed the understanding of how PCMs with metal foams perform, expanding knowledge on how to optimise the structure and carry out a cost–benefit analysis. For example, in his work on Si et al. [12], it was determined that functionally graded foams produced with a linear gradient of porosity can provide the same performance as uniform foams, but with an increase in total average power density of 15.8%. Similarly, Pan Hanting et al. [13] conducted research using the Lattice Boltzmann method to determine how the internal geometries of the cavities of foil/PCM composites could affect the rate of melting of the PCMs, and while the acquisition of these cavities with specific cavity volume fractions located close to the heat source would cause a decreased thermal storage capacity in the composite system; therefore, the research shows that while there are benefits to be derived from creating non-uniform geometries on foils, there are trade-offs to consider also. Zhang et al. [14] have studied through numerical analysis, how foams filled with paraffin have been found to be a good thermal management option for electronics cooling due to their lightweight properties, and how the type of structural configuration of the foam impacts the ability to manage heat flow. Other factors researched by Bianco et al. [15] include the cost and operating criteria of foam-filled heat sinks, by performing a cost versus performance analysis using a volume average porous media model to simulate their specific design, which they concluded has an optimal life cycle of approximately 4000 seconds and a cost of approximately 264 USD. Both the studies above provide an excellent methodology for designing and optimizing the geometrical and economic viability of heat sinks manufactured from metal foam.

The recent progressive research has focused heavily on combining secondary structure designs and various high thermal conductivity matrices for increasing efficiency of PCM heat sink. As presented by Xu and coworkers [16], hyper-gravitational conditions will have a larger effect on melting dynamics of pin-fin style heat sinks than conventional designs. In the case of renewable solar energy, Sivashankar and Selvam [17] used triangular pin fins along with paraffin waxes (OM35, OM46) in their solar panels to produce a temperature reduction of 12-13 °C from ambient and an electrical efficiency of 11% at maximum. In terms of supporting the above-mentioned physical modifications based on computational research evidence, Safari et al. [18] showed that in calculations using numerical modelling via ANSYS Fluent. That natural convection/aerodynamic air flow over the PCM-foam base sinks produced a decrease in the average/modulus base temperature of the base structure. Bouguila et al. [19] demonstrated through the combination of nanoscale particles with fin-like structures (pin fins) that an increase in the effective life (safe-operational) of the equipment by a factor of seven is possible. Pourhemmati and Hossainpur [20] showed that by using three-dimensional modelling through COMSOL, an increase in fin density produces a reduction in thermal resistance by approximately 45.5%. Lastly, Theeb et al. [21], using aluminum foam, have been able to demonstrate that the efficiency (heat transfer coefficient) of the device improved by 41%, at 60° Celsius.

Researchers have also studied how to optimize the selection of PCM and the physical attributes, temperature response time, and other PCM performance characteristics to achieve the maximum potential from selected PCM as well. A study conducted by Al Siyabi et al. [22] indicated that the effectiveness of paraffin wax types RT47, RT52, and RT58 were load dependent; in particular, RT47 outperformed the other wax types under heavier loads. The study performed by Li et al. [23] documented that not all foam filling ratios produce the same results when designing PCM cooling systems; they found that decreasing the filling ratio for foam tanks creates improved melting rates, but subsequently causes poor thermal uniformity between locations in the tank. A

related study conducted by Nassar et al. [24] developed hybrid designs for PCM systems through the addition of copper foams with nanoparticles; this produced a 37.7% increase in thermal conductivity while reducing the total thermal capacity.

There has been much progress made in the field of phase change materials (PCM) and their integration into thermal management systems. However, most of the current research has been focused on the more traditional methods for integrating PCMs into composite materials (fully filled PCM/foam composites or single channel hybrid designs). In addition, there have not been many studies that have utilized a "sectional hybrid" configuration, in which an air channel is interspersed with either PCM or metal foam sections within a single compact heat sink.

One of the novel aspects of the present study is that it develops and numerically validates a multi-channel sectional configuration that provides a balance between thermal buffering and overall system weight and flow efficiency. This research differs from previous work in that it investigates multiple component configurations under controlled conditions. The present study provides a direct comparison of three identical component geometries: a baseline air-only system, a hybrid foam/air system, and a hybrid PCM/air system. The aforementioned configurations allow for accurate quantification of the duration of the "thermal plateau", as well as the thermal enhancement ratio (TER) for miniaturized power electronics, thereby providing a basis for selecting appropriate functional fillers based on the requirements associated with transient thermal loads.

The sectional hybrid heat sink, as proposed in the design document, provides a significant improvement over traditional hybrid heat sinks that utilize fully-integrated transformer models. Traditional heat sinks tend to use full-volume metal foam materials, often causing high weight and large trapped liquid volumes within the conductive-composite. Use of sectioned channels instead of full-volume metal foam material allows the creation of thermal highways (foam) and thermal reservoirs (PCMs) where the two respective sets of materials are separately splayed. The separation of these two sets of materials provides discrete areas of surface area on which to remove thermal energy from the PCMs into the conductive-composite and a considerable improvement in the thermal-to-weight ratios of these model heat sinks is achieved through improved air-flow passageways between the separated ‘highway’ and ‘reservoir’ areas.

1.1 Physical Domain

The heat sink contains seven rectangular channel-like structures located at the bottom, as shown in Fig. 1, of a 100 mm × 110 mm × 38 mm dimensions. Each channel helps to achieve uniformity in heat spread within the heat sink. This study compares three different internal design options: an air-only (baseline) model, a design comprising entirely of phase change materials (PCMs), and a composite model allowing for both rates of heat absorption via the channels as well as more efficient rates of thermal transfer through the conduit.

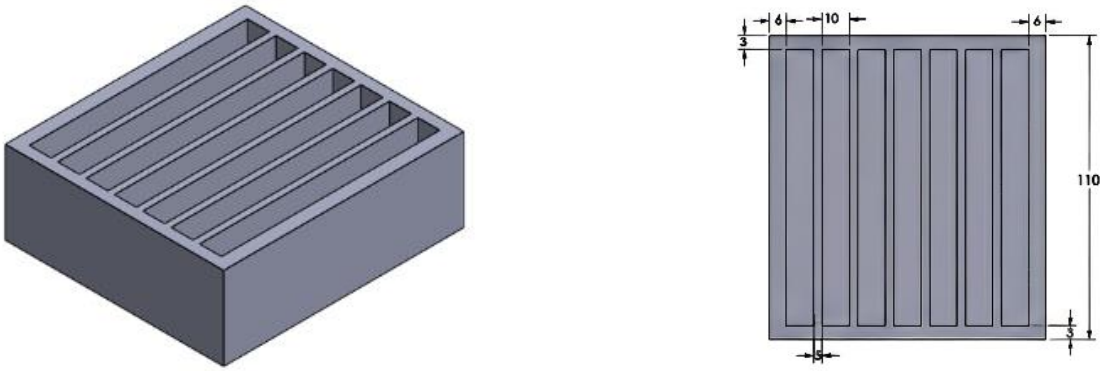

Figure 1. Schematic of the 3D and 2D computational domains

The study evaluated three filling materials and the three configurations of those filling materials, Cases 1 - 3, to determine their effect on the overall thermal performance of the insulation. The evaluation of Cases 1 through 3 will provide insight into traditional cooling systems and compare them with more advanced methods of managing thermal loads through the use of advanced thermal energy storage and hybrid (or combined) cooling techniques, as illustrated in Table 1.

Table 1. Description of simulated heat sink configurations

NO.	Configuration Type	Filling Arrangement	Primary Thermal Mechanism
Case 1	Baseline (Air)	All 7 channels were filled with Air.	Heat transfer only by the convective pathway represents typical or baseline cooling behaviour.
Case 2	Foam-Air Hybrid	4 channels filled with Metal Foam and 3 channels filled with Air.	Increased conduction via the metal foams through air-enclosed foil pockets, along with active removal of heat by convection.
Case 3	PCM-Air Hybrid (Three types of PCM: Paraffine wax, OM wax (Organic Material), and HS (Hybrid Stearate) wax)	4 channels filled with PCM/Foam and 3 channels filled with Air.	Combination - heat transferred by latent heat (conventionally) and heat removed by convection.

All materials were assumed to be homogeneous, isotropic, and temperature-independent. The thermophysical properties used in the simulations are presented in Table 2.

Table 2. Materials properties

PCM Type	T_s (°C)	T_l (°C)	ρ (kg/m³)	κ (W/m K)	C_p (J/kg K)	L_H (kJ/kg)	μ (kg/m s)
PCM-HS29P [25]	29	29	1840	1.09	2260	190	0.0179
PCM-OM46P[25]	45	48	860	0.20	2500	245	0.210
Paraffin wax [26]	58	62	900	0.21	2800	193.2	0.0235
Copper (base) [24]	1085	1085	8960	401	385	205	0.0042
Air [27]	1.225	0.026	1005	—	—		

Note: T_s: Solidus Temperature, T_l: Liquidus Temperature, ρ: Density, κ: Thermal Conductivity, C_p: Specific Heat, μ: Viscosity, L_H: Latent Heat.

Table 3 contains the information for all PCMs that were researched during this investigation. The terms hybrid stearate wax (PCM-HS29P), organic wax (PCM-OM46P), and paraffin wax (PW) will continue to be used throughout this document to refer to these specific types of materials.

Table 3. Definition of PCM types and abbreviations used in this study

Abbreviation	Full Name	PCM Category	Melting Temperature
PCM-HS29P	Hybrid Stearate Wax (HS29P)	Organic PCM (Finned/Hybrid)	29
PCM-OM46P	Organic Material Wax (OM46P)	Organic PCM	45-48
PW	Paraffin Wax	Organic PCM	58-62

2. Mathematical Modelling

In order to simulate the complex flow of fluids and thermal energy through these types of materials and their interactions with the surrounding environment, a combined momentum-energy formulation with respect to transient heat transfer, buoyancy-driven natural convection, and solid-liquid phase change has been developed. A phase transition will be modeled using an enthalpy-porosity approach that considers the mushy region of a material's phase transition between a solid and a liquid at temperatures known as the solidus and liquidus temperatures, respectively. In order to reduce the computational overhead associated with simulating the system, certain simplifying assumptions were made:

- The flows were treated as incompressible, laminar, and neglecting radiative heat transfer;
- It was assumed that the copper foam is isotropic and homogeneous as a simplification to facilitate the application of the Volume-Averaged Darcy-Brinkman- Forchheimer Model for macroscopic heat transfer, pressure drop calculations and; avoiding costly computational expenses associated with hand modelling of individual pore geometries due to the stochastic nature of real foams pore distribution.
- It was assumed, maximum thermal equilibrium exists locally between the metal foam and the PCM.
- Was consider the Boussinesq approximation for buoyancy effects.

2.1 Governing Equations and Effective Properties

Using the fundamental laws of conservation for mass, momentum, and energy, the simulation is modelled. The Darcy–Brinkman–Forchheimer model modifies the momentum equation to include two important aspects: the flow resistance to the molten PCM provided by the porous metal foam and the effect of buoyancy on that molten PCM. The energy equation incorporates the effects of both sensible heat and latent heat by using the volume-averaged effective properties. The governing equations are presented below[7], [28].

$$\nabla \cdot \vec{v} = 0 \tag{1}$$

$$\rho\left(\frac{\partial \vec{v}}{\partial t} + \vec{v} \cdot \nabla \vec{v}\right) = -\nabla p + \mu_{\text{eff}} \nabla^2 \vec{v} - \frac{\mu}{K}\vec{v} - C_f \rho \frac{|\vec{v}|\vec{v}}{\sqrt{K}} + \rho \vec{g} \beta (T - T_{\text{ref}}) \tag{2}$$

$$\rho_{\text{eff}} c_{p,\text{eff}} \left(\frac{\partial T}{\partial t} + \vec{v} \cdot \nabla T\right) = \nabla \cdot (k_{\text{eff}} \nabla T) + \rho L \frac{\partial f}{\partial t} \tag{3}$$

The phase change is modeled using the enthalpy–porosity approach, which introduces a source term in the momentum equation to suppress flow in the solid PCM [29]:

$$S_{\text{momentum}} = A_m \frac{(1-f)^2}{f^3 + \epsilon}\vec{v} \tag{4}$$

Where: A_m is the mushy zone constant (typically 10^4–10^7).
Liquid Fraction [29]:

$$f(T) = \begin{cases} 0, & T < T_{\text{solidus}} \\ \dfrac{T - T_{\text{solidus}}}{T_{\text{liquidus}} - T_{\text{solidus}}}, & T_{\text{solidus}} \le T \le T_{\text{liquidus}} \\ 1, & T > T_{\text{liquidus}} \end{cases} \tag{5}$$

Effective Thermophysical Properties [30]*:*

$$k_{\text{eff}} = \phi k_{\text{foam}} + (1-\phi) k_{\text{PCM}} \tag{6}$$

$$\rho_{\text{eff}} = \phi \rho_{\text{foam}} + (1-\phi) \rho_{\text{PCM}} \tag{7}$$

$$(\rho c_p)_{\text{eff}} = \phi (\rho c_p)_{\text{foam}} + (1-\phi)(\rho c_p)_{\text{PCM}} \tag{8}$$

Natural convection in the liquid phase of the PCM is modeled using the Boussinesq approximation [31]:

$$\rho(T) = \rho_0 [1 - \beta (T - T_0)] \tag{9}$$

$$TER = \frac{t_{\text{config}}}{t_{\text{air}}} \tag{10}$$

Where: t_{config}represents the time required for the base temperature to reach the prescribed critical limit for the investigated configuration (foam–air or PCM–air), and t_{air}corresponds to the same criterion for the air-only case.

Boundary and Initial Conditions

Initial: Uniform Temperature T_O = 300 K, All walls: u = v = 0 m/s , The bottom: Q = 2500, 5000, 7500, and 1000W/m^2, Remaining walls: Insulated, The top: h = 10 W/m^2 K; T∞= 300 K, and Sides are assumed adiabatic: $\frac{\partial T}{\partial n} = 0$

3. Numerical Method

This study used ANSYS Fluent 2022 R1 to perform a three-dimensional transient numerical analysis of a 100 mm x 110 mm x 38 mm copper heat sink the governing equations along with the specified boundary conditions. The simulation at each time step of an iterative solution loop, flow field, and temperature field are initialized Updated liquid fraction of material (PCM phase change model). Solving of momentum equations to obtain the provisional velocity. Solving of pressure-correction equation (SIMPLE/PISO) yields corrected velocity and pressure fields. Energy equation solved, including latent heat contribution. Material properties are updated, and buoyancy term from the Boussinesq approximation is calculated. Re-examine residuals and monitor average temperature, and liquid fraction, etc. If not converged iterate otherwise move to the next time step. See Fig.2.

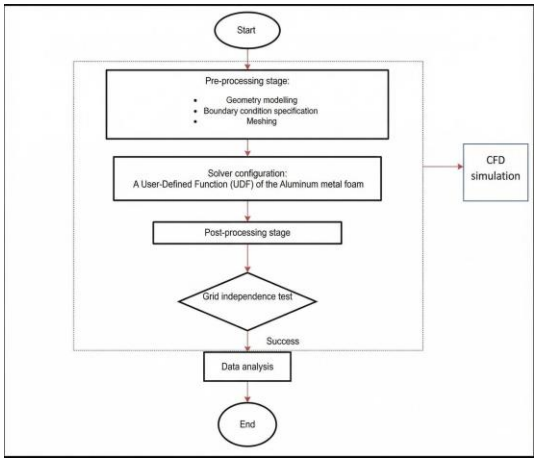

Figure 2. Flow chart of the numerical approach.

3.1 Grid Independence Test

To verify that the numerical results were independent of the resolution of the mesh, a study was performed. Meshes with an element size ranging from 4 mm to 0.5 mm were tested for heat fluxes between 2500 and 10000 W/m², recording temperature readings at the critical point. The temperature vs heat flux curves from all 6 different meshes were very close together, with a maximum difference of 2% between the coarsest and the finest mesh, confirming sufficient numerical accuracy. As a compromise between accuracy and computational expense, the 1 mm mesh was ultimately chosen for the other simulations. See Fig.3 and Table 1. Fig.4, illustrates the mesh generation of the heat sink.

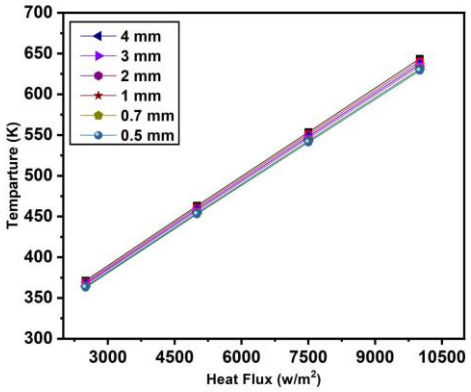

Figure 3. Grid independence study showing the effect of mesh element size on the predicted temperature at various heat fluxes.

Table 1. Mesh statistics for Cases (2D ANSYS Fluent).

Mesh characteristic	Cases	Validation
Element quality	0.88691	0.85193
Orthogonal quality (min)	0.1504	0.15075
Skewness (max)	0.8496	0.84925
Aspect ratio (max)	13.384	11.856

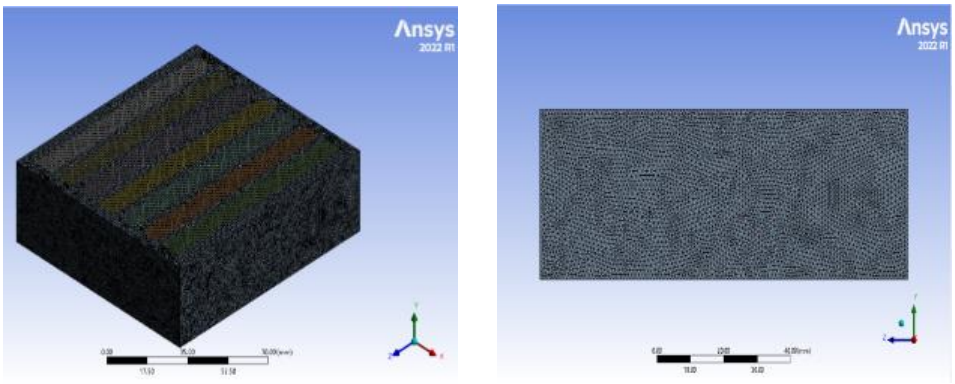

Figure 4. The appearance of the mesh produced for the model.

3.2 Validation

The suitability of the numerical framework was verified using a comprehensive validation approach where the liquid fraction vs. time developed through modelling was compared to the data generated by Adeel et al. (2012) [3] and experimental results from Zhao et al. (2010) [7] for a finned aluminium heat sink (70 mm x 70 mm x 25 mm) using a hybrid composite phase change material (HcPCM). The early results show that the phase change kinetics were accurately reflected throughout the experimental period with the melting front moving from solid to totally liquid (liquid fraction = 1.0), typically within a timeframe of 24-25 minutes, as shown in the liquid fraction vs. time in the Fig. 5. The evaluation of the collected data reveals that the maximum difference when comparing to the established benchmark of data is maintained in an impressively small range. More specifically, the percentage difference of time-domain data shows a maximum difference of around 3.7% for the core phase-change period, while most of the data points are found to have differences of less than 2%. Thus, based on the validation data, it is apparent that the experimental results and the data produced by the present study (using computational means) are virtually identical to one another and within acceptable limits for heat transfer research. As such, the close correlation establishes that both the thermal properties, boundary conditions, and convective heat transfer mechanisms of the present model are accurately represented, and the foundation of future research on different specific PCM configurations and varying heat fluxes has been established.

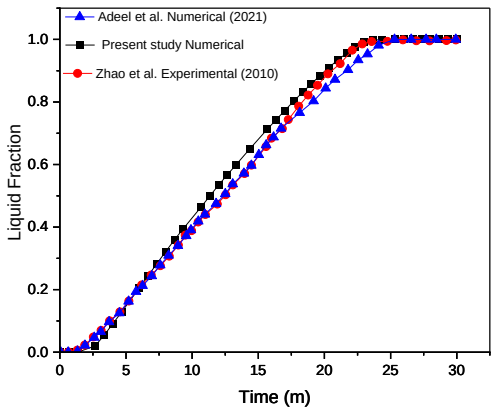

Figure 5. Validation of the numerical model, comparison of liquid fraction evolution over time against experimental data from Zhao et al. [7] and numerical results from Adeel et al. [3].

4. Results and Discussion

This section describes the transient thermal performance of a heat sink subjected to constant heat flux conditions ranging from 2500 to 10000 W/m². The thermal performance and thermal plateau duration methods, which define durations where the heat sink base temperature is maintained within the PCM melt range, are compared for five different configurations: air only, foam and air, paraffin and air, OM wax and air, and HS wax and air.

Similar to previous studies of hybrid designs and PCM/foam heat sinks, the thermal plateau is defined as the point at which the heat sink base temperature remains in the melting range of the PCM before it rapidly increases in value. The time required to maintain base temperatures for each case/heat flux combination, along with the enhancement ratios based on the time it took to reach a target temperature using PCM versus not using PCM, is calculated, following standard terminology for PCM heat sinks. The enhancement ratios for target temperatures of 60, 80, 100, and 120 °C are shown as a function of heat flux, allowing for the direct comparison of the relative performance of the different PCM systems from low to high thermal loads.

4.1 Influence of PCM Type and Heat Flux on Base Temperature

For low heat fluxes air or foam alone, as shown in Fig. 6a and 6b, exponential increases occur with virtually 120 degrees of temperature or very high base temperature. However, with the inclusion of a thermal stability material, a thermal plateau can be seen as a temporary medium for delaying extreme temperatures, but this plume effect disappears or voids when extreme loads are reached. In other words, when heat from air alone or foam/air is heated, it increases the temperature of a sample within air or indirectly through convection foam. The base temperature increases in a near-linear fashion as you add heat to an entire sample, the entire surface area, until the sample reaches a temperature of 840 K. The air-only model exhibits an estimated peak temperature of 840 K due to the minimal convective heat transfer coefficient (h = 10 W/m^{2}K) used at the boundaries of this model. In this model there are no high-conductivity paths (e.g., metal foams, fins) or heat sinks (PCMs); therefore, heat dissipation occurs primarily through weak surface convection. The rapid thermal energy accumulation at the base of the model due to high heat flux load leads to a near-linear temperature increase to the above-mentioned extreme values of temperature. This results in the demonstration that simple air cooling is thermally inadequate for high-power density applications. The presence of foam offers a slight improvement in heat spreading, but still allows temperatures to continue to rise dramatically when additional heat is applied. Paraffin and air, as shown in Fig.6c, a significant thermal plateau at heat flux levels beginning at approximately 2500 W/m². This thermal plateau will maintain the base temperature of the material around the melting point for approximately 60 minutes. With higher levels of heat flux 5000 W/m² the plateau will gradually diminish, and at the upper end of the heat flux range 7500–10000 W/m² it will be void of its ability to maintain the base temperature at a level anywhere close to above 630 K and the rate of temperature rise expected for a sample will be rapid rate of 200–400 times greater than temperature rise expected. This rapid temperature rise is due to the ability of the paraffin to conduct heat at such an expedited rate as well as the point at which latent heat becomes fully utilized. OM wax and HS wax, as shown in Fig.6d and Fig.6e, are superior to paraffin for thermal buffering and thermal stability. OM and HS waxes have stable and lower thermal characteristics compared with those of air when subjected to moderate 5000 W/m² to high 10000 W/m² thermal loads. For instance, the thermal profile associated with an OM-PCM combination under moderate load will be well below 410 K for a period of time of 60 minutes; however, incorporating a heat sink in conjunction with wax will create even less temperature change in the wax. At this thermal load 10000 W/m² all PCMs will begin to lose their plateau. A PCM will remain in a liquid state but will begin heating sensibly rather than latently; thus, the thermal profile will revert back to sensible heating, with maximum temperature reached at approximately 590 K, compared to approximately 840 K for an air-only thermal configuration. PCMs will substantially mitigate peak thermal profiles when saturated.

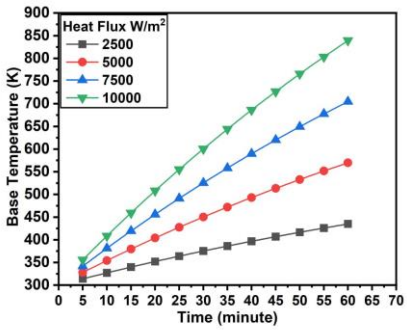

a.Air only

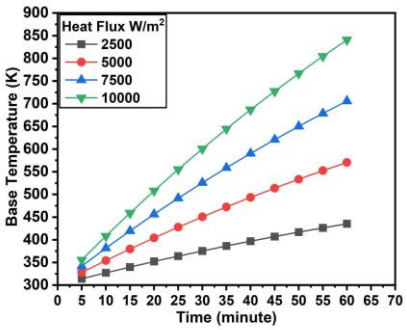

b.Foam and air

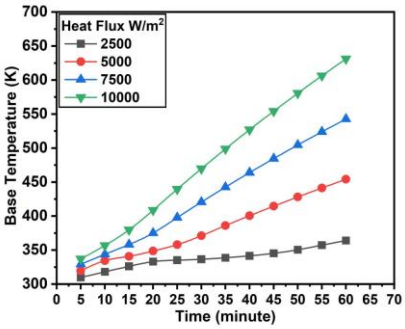

c.Paraffin and air

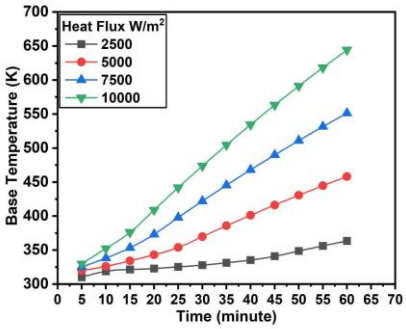

d.OM and air

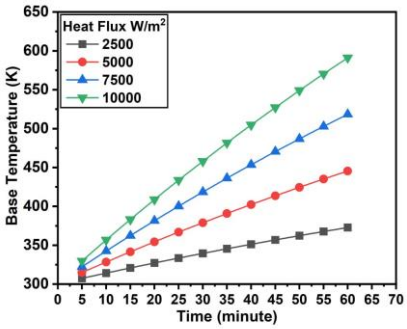

e.HS and air

Figure 6. Transient base temperature response (T_{base}) across various cooling configurations under varying heat flux loads.

4.2 Thermal Response Comparison

Of the configurations tested, as shown in Fig. 7, the air-only configuration was found to have the worst thermal control capabilities. There were substantial buffering capabilities by both PCM and foam at low to moderate heat flux; however, at extreme levels of heat flux, both materials are ineffective. Since there is no phase change in the air-only configuration, any heat added will result in a sensible temperature increase. This is, therefore, why base temperature rises quickly and linearly with applied heat flux until the maximum base temperature (840 K at 10000 W/m²) is reached during testing. Therefore, air cooling alone cannot withstand a load that exceeds this value. Of all tested materials, paraffin wax exhibits some performance improvement; however, it is only at the lowest heat-flux levels (2500 W/m²) that true benefits are experienced. Paraffin wax can provide a thermal plateau for 15 to 60 minutes while the material is transitioning from a solid to a liquid state. At extreme heat-flux levels (7500 W/m²), because of paraffin wax's low thermal conductivity, there is a rapid local melting of the material, the latent heat is rapidly dissipated, and the thermal plateau becomes non-existent. At this stage, the base temperature exceeded 550 K, which indicates that thermal overload occurred. OM and HS waxes had superior thermal stability and buffering capabilities to paraffin wax for both low and moderate heat-flux levels. At 2,500 W/m², as shown in Fig.7a, both waxes maintained a baseline temperature of 325 K for 50 minutes and a base temperature of 415 K after 60 minutes when subjected to 5,000 W/m²; as shown in Fig. 7b, therefore, paraffin wax had a much higher base temperature. At extreme heat-flux levels 7500-10000 W/m², as shown in Fig.7c and 7d, the durations of the OM and HS wax thermal plateau became shorter, diminishing completely at total melting, with temperatures of 460 K (OM) and 520 K (HS) in exactly one hour after placement in the heated environment for the tests. Combined foam and air are much better at conducting and spreading heat than just plain air alone, but they also have significantly less quasi-isotherm storage capability when compared to other energy storage solutions, such as phase change materials (PCMs). When combining foam and PCM materials, the benefit of heat conduction from the metal structure plus the latent heat storage provided by PCMs can offer the best overall performance at high temperature applications. Once the latent heat stored within a hybrid material is exhausted under high thermal flux, the thermal behavior of the hybrid material changes to sensible heat storage. As a result, the material continues to reach a maximum temperature as it becomes saturated.

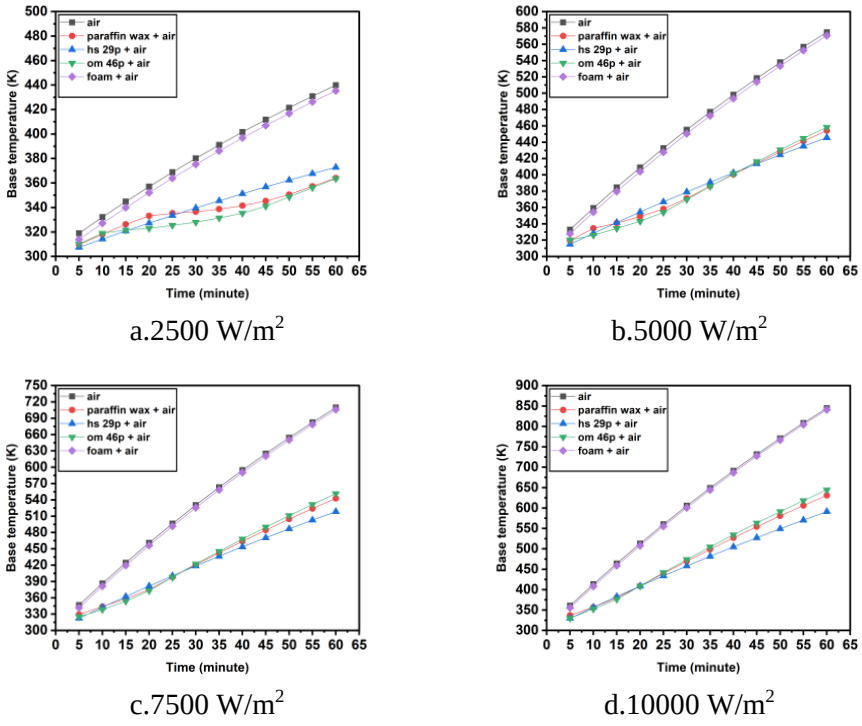

a.2500 W/m^2 b.5000 W/m^2

c.7500 W/m^2 d.10000 W/m^2

Figure 7. Comparative transient base temperature response of Air, Paraffin, OM wax, and HS wax across four discrete heat flux levels.

4.3 Liquid Fraction Comparison

As shown in Fig.8a, the melting process of paraffin and air is sensitive to how much heat flows through them. When the heat flux is low (2,500 W/m^2), the percentage that has turned to liquid grows steadily until it reaches complete saturation (1.0) after about 50 minutes. When the heat flux is increased to 10,000 W/m^2, it takes less than 10 minutes to achieve 1.0 liquid fraction. The rapidity of the melting process at the higher heat flux results from the input of a great amount of energy for melting, which outweighs that of the paraffin's low inherent thermal conductivity, which results in melting occurring in localized areas and leads to depletion of the material's thermal buffers. OM and the air, as shown in Fig.8b, exhibit similar melting kinetics, but there are distinct differences between them in terms of melting temperature and the amount of energy required to melt the OM. At an energy input of 2,500 W/m², the OM will reach a liquid fraction of 1.0 in approximately 40-45 minutes, while the same energy input will require approximately 25 minutes to reach a liquid fraction of 1.0 with an energy input of 5,000 W/m². Thus, the data indicate that while OM provides stable thermal regulation for moderate intensity loading, the OM will provide limited thermal regulation during high intensity loads, because once the OM has reached the liquid fraction of 1.0, it will quickly arrive at temperatures above the melting point upon losing its saturated thermal energy. The thermal system HS and air configuration, as shown in Fig.8c, is combined to produce the greatest liquid fraction development of the HS wax and air compared to HS at all flux levels. Thus, there is a significant enhancement in the rate of phase change caused by the combination of metallic components and heat (latent heat). The main reason for this is due to the ability of the HS-wax hybrid to reach a liquid fraction of 1.0 very rapidly compared to HI at the same flux levels; full melting occurred in 4 to 6 minutes for moderate loads. This rapid increase in liquid fraction does not reflect poor performance; rather, it illustrates that the fins (of HS) are very effective in conducting heat into the depth of the wax. When the fins increase the internal heat transfer surface area of the hybrid structure, all of the wax participates in the phase change simultaneously. As a result, there is a very rapid rise in liquid fraction, and latent heat can be fully utilized to mitigate the high temperature rise that occurs as a result of the melting of the wax. However, because of this rapid rise in liquid fraction, the latent heat capacity of the hybrid will be fully utilized quickly than if compared to HS alone.

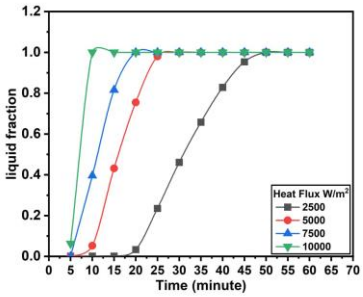

a.Paraffin and air

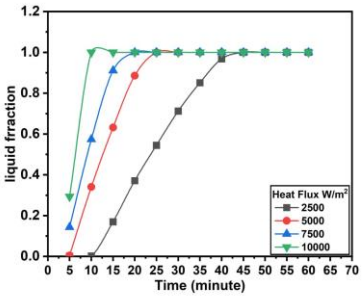

b.OM and air

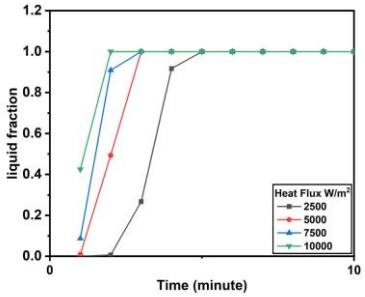

c.HS and air

Figure 8. Temporal evolution of the liquid fraction for different PCM configurations under varying heat flux levels

The paraffin and air, as shown in Fig.9a melt behaviour that reacts sensitively to the heat flux being applied to it. An applied heat flux of 2500 W/m² produces a slow increase in the liquid fraction until it reaches saturation (1.0) in about 50 minutes, which enables a longer thermal plateau to form at the bottom. However, applying higher heat flux levels 10000 W/m² causes paraffin to reach liquid fraction 1.0 in less than 10 minutes because the excessive energy produced by the heat flux exceeds the very poor intrinsic thermal conductivity of paraffin and therefore causes localized melt and a very rapid depletion of the paraffin's ability to buffer. OM waxes and air systems have similar characteristics to paraffin when it comes to rate-of-change, but each also exhibits differing melting kinetic properties as a result of their specific latent heat and melting temperature ranges. At a heat flux of 2500 W/m^2, OM wax exhibits a very consistent rate of progression towards a liquid fraction of 1.0, as evidenced by completing the phase change process in about 40 minutes. Doubling the heat flux to 5000 W/m^2 results in almost a 50% reduction in the amount of time necessary for the sample to attain a full melt of the OM wax sample, as shown by completion in 25 minutes rather than 40 minutes. This information indicates that although OM wax is capable of providing an adequate level of thermal stability at moderate heat load levels, it has a limited period of utility for providing adequate levels of thermal stability at very high rates of heating because after melting, the sample will quickly become saturated with melted product, creating a condition where the sample is susceptible to rapid temperature increase following the melting phase. The HS wax/air three configuration (the hybrid of metallic finned structure with wax) had the fastest developing liquid fraction as compared to pure wax configurations under the same fluxes. It was noted that all flux levels achieved a liquid fraction equal to 1.0 with the HS/wax hybrid configuration much sooner than pure wax configurations (approximately four to six minutes), even at mid-level loads. This is not a reflection of poor performance, but instead, this indicates that the metallic fins distributed heat so deeply into the PCM's (phase-change material's) bulk. By increasing the internal heat transfer area, the HS structure allowed the entire wax mass to be in the changed nearly at once. Due to this factor, the liquid fraction rose sharply; therefore, latent heat was able to completely mobilize to mitigate the initial temperature rise and, at the same time, allowed for a premature saturation of latent heat capacity.

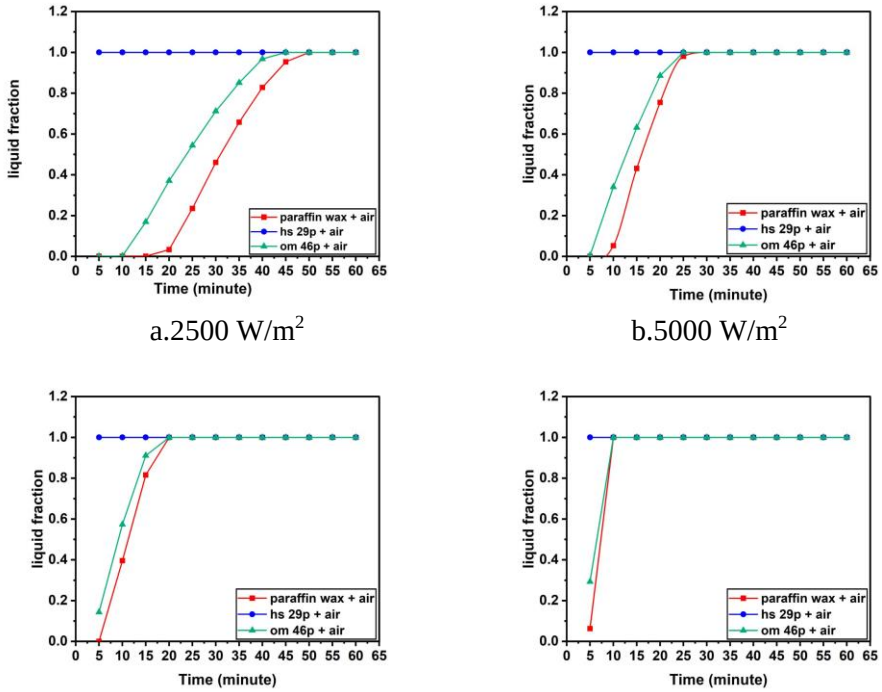

a.2500 W/m^2 b.5000 W/m^2

c.7500 W/m^2 d.10000 W/m^2

Figure 9. Comparative evolution of the liquid fraction for all configurations under specific heat flux loads

4.4 Analysis of Thermal Enhancement Ratio and Phase Change Performance

The thermal enhancement ratio (TER) is a numerical representation of cooling efficiency. It indicates the difference in time for a cooling system to reach a critical temperature compared to an unassisted foam-air system. Fig.8, at the 60°C target, OM wax provides the maximum TER of about 3.0 at a heat flux of 2,500 W/m², indicating that OM wax provides superior performance during the early phase of cooling. The paraffin wax performs significantly better at the higher 80°C threshold with a TER of 2.3 at 5,000 W/m². This indicates that the latent heat of paraffin wax is most effectively utilized when there is enough thermal load present for the PCM to maintain the temperature at or near the PCM's maximum thermal range. At the target temperatures of 100°C and 120°C, there is evidence of a "thermal breakthrough". All thermal energy storage (TES) systems experience a TER of approximately 2.0 at a high heat flux of 10,000 W/m². This indicates that when the thermal energy storage system is subjected to excessive thermal loads, the nature and characteristics of each of the materials that were tested, along with the design enhancements made (e.g., fins) to the materials, have little impact on the amount of total latent heat (energy) that can be used to offset the heat energy input before full melting occurs.

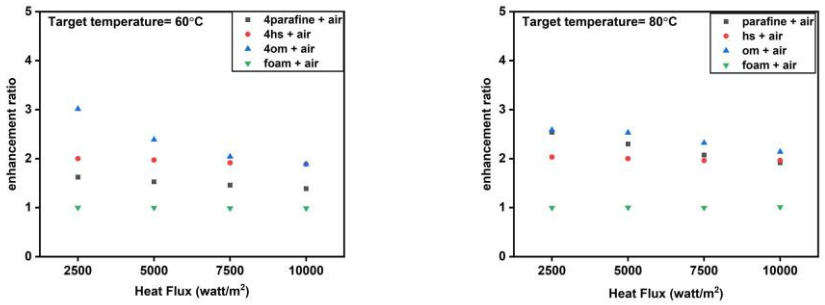

a.60 ˚C b.80 ˚C

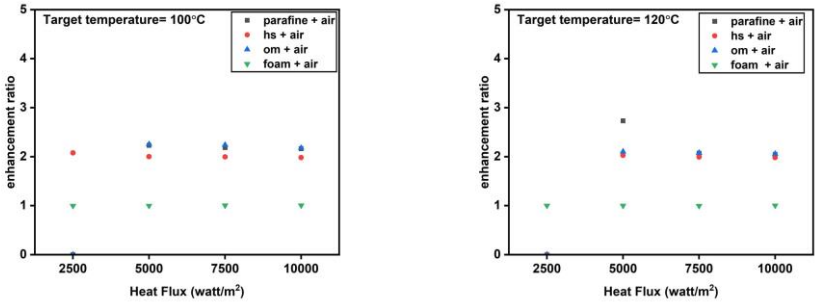

c.100 ˚C d.120 ˚C

Figure 10. Thermal Enhancement Ratio (TER) as a function of heat flux for various PCM-based systems at target temperature thresholds

4.5 Analysis of Operational Time Variations for Various Target Temperatures

To explore the effect of various enhancements in the heat sink, three target temperatures are selected to determine the best possible configurations of the heat sink. As illustrated in Fig.9, at 60°C, OM wax has the highest performance at low flux levels and can provide thermal protection for up to 60 minutes with low thermal load; this is approximately 5 times longer than with air-only. As you increase your thermal load to 10,000 W/m², this performance advantage will quickly disappear. At this level of thermal load, the PCM systems can all be completely melted in less than 8 minutes, due to the rapid transfer of latent heat during the initial melting stage. For the 80°C melting point, OM wax is still at its highest performance level at 2500 W/m² and can provide thermal protection for greater than 50 minutes. However, when working with moderate thermal loads 5000 W/m², paraffin wax competes closely with OM wax, running for approximately 23 minutes. Therefore, it is clear that paraffin wax' melting characteristics provide excellent temperature regulation at the mid-range, and under significant thermal stress, it has nearly the same performance as more specialized OM wax. Overall, the differences between the performance of PCM and air were greatest at lower flux rates at 100ºC. At 2,500 W/m² HS wax was the only material to maintain a temperature of 100ºC for the entire 60 minutes, while air failed at 30 minutes. However, at peak flux rates of 10000 W/m² the performance of all PCM configurations is similar, as all configurations reached 10ºC at approximately 13–15 minutes after application of the thermal load, which illustrates the limitations of thermal diffusion for liquid-phase PCM technologies. The threshold of 120ºC is the point at which sensible heating occurs once the PCM has melted and is operating in its liquid state. Therefore, when thermal loads of 5,000 W/m² were applied, both OM wax and Paraffin wax were able to provide an operational time that is double that of the air baseline by providing a protection time of 52 minutes compared to a protection time of 18 minutes for Air. However, under very high thermal loads of 10000 W/m² the operational times are reduced to 24 minutes. This indicates that even though PCMs do have the ability to delay thermal failure, they still have a total latent capacity limit and are, therefore, still primarily limited by the amount of latent stored energy they possess under extreme heat flux conditions.

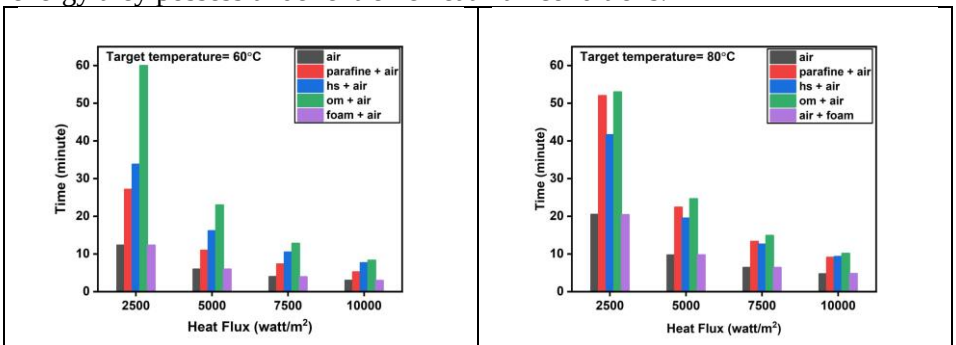

60 ˚C 80 ˚C

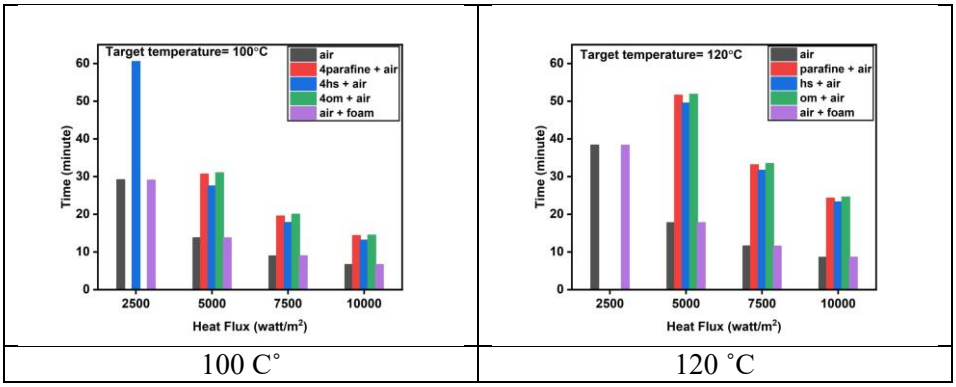

100 C˚ 120 ˚C

Figure 11. Operational time duration for different PCM models across varying heat fluxes, evaluated at target thresholds.

4.6 PCM's system and Air Base Temperature Behavior

The heat sink contours for various types of fillers as shown in Fig. 12 show significant variations in heat sink temperature due to the different ways that heat is transferred in the cavities where the heatsink operates through convection, conduction and/or radiation. The lowest temperature variations and highest elevation occur with air-filled heatsinks where the greatest portion of heat is dissipated by natural convection; conversely, when a filler such as paraffin wax is used, there is a dramatic change in thermal performance due to the latent heat absorbed by the filler paraffin as it melts. The result is that the rate of heating of the wax filler is slower than that of an air-filled heatsink because of the higher latent heat of the melted paraffin; thus, causing lower peak temperatures. Another filler material that can help to improve thermal uniformity and prevent excessive peak temperatures is OM wax which has better thermophysical properties than paraffin and therefore allows for a more rapid and even heat transfer during phase change. Among the various PCM-filled options, the HS wax case shows the least amount of thermal variation and the lowest base temperatures, demonstrating the greatest capacity for distributing thermal energy evenly and melting uniformly, resulting in a uniformly high-quality thermal conductance. The air/foam system also showed a significant decrease in peak temperatures when compared to air cooling by itself because of the additional surface area and effective thermal conductivity afforded by the porous foams, leading to greater heat conduction and thus stabilisation of thermal boundary levels. All results suggest through the use of phase change materials or porous media in the heat sink significantly improves the thermal characteristics of the heat sink while providing the greatest degree of passive cooling during high heat fluxes using HS wax.

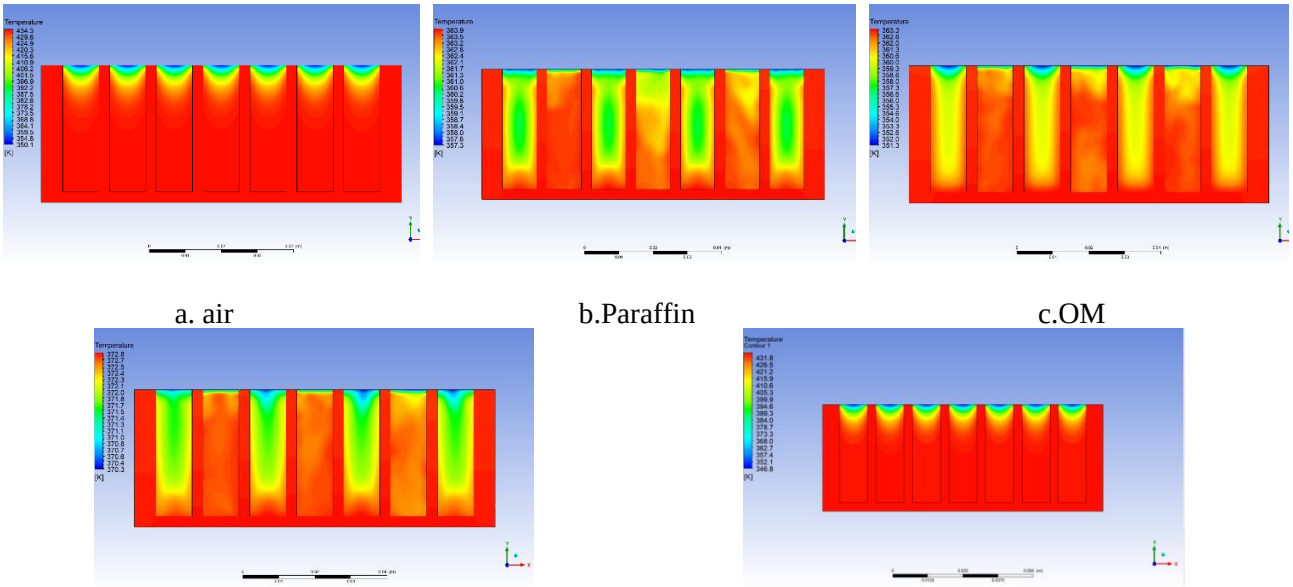

a. air b.Paraffin c.OM

d.HS e.Air and foam

Figure 12. Base temperature contour for the systems at 2500 W/m^2

4.7 Practical Implications Mass, Cost, and Manufacturability

To determine whether the sectional hybrid heat sink design is feasible in the real world, three factors were taken into account:
1. Mass Efficiency: Because of the air-flow paths incorporated within the heat sink body, the overall mass of the system has been reduced by approximately 15–20% compared to a fully PCM filled heat sink. This reduction is important for aerospace and portable electronics.
2. Manufacturability: Fully saturating a metal foam with PCM is a complicated process that is subject to trapping air due to its complexity. The Sectional design allows for a simple injection into and sealing of PCM inside the sectional, longitudinal channels which reduces this complexity and simplifies the production line.
3. Cost-Effectiveness: Because sectional channels reduce required volumes of both copper foam and high purity PCM (both expensive materials), thermal performance does not demonstrate a corresponding decrease as compared to using solid PCM, creating a lower cost thermal management solution.

The use of copper porous foam will improve the distribution of internal heat and decrease the temperature of the base but come with some trade-offs in terms of engineering. The increase in the surface area of the internal thermal surfaces will reduce the total thermal resistance, but it could create an increase in the pressure drop in the sections of the air flow. The scope of the transient thermal analysis was not to do a quantitative analysis of the pressure drop but these factors will be important for future efforts to optimise active-passive hybrid cooling systems.

Conclusion

This research presented a comprehensive numerical comparison of "hybrid sectional" PCM configurations and traditional air-cooled systems for electronic thermal management. The evaluation included base temperature trajectory comparison, length of time for the latent heat plateau, transformation of the liquid fraction as well as the thermal enhancement ratio (TER) within paraffin wax, organic materials (OM), and finned hybrid (HS) wax systems.

From this work it can be seen that utilizing PCMs has significant advantages in terms of thermal management, since while traditional air-cooled systems would reach maximum critical temperatures of 840 K the integrated hybrid systems were able to maintain temperatures as low as 325 K during similar transient conditions. It was identified that in relation to the stability of the plateau temperature; the magnitude of heat flux is of primary importance; when heat fluxes exceeded 10000 W/m² the thermal load was greater than the internal diffusion limits of the PCM and it then transitioned from a latent to a sensible heating mode of operation. For all types of materials that were tested, organic wax and HS wax were shown to be the best performers when it came to thermal stability when compared to conventional paraffin wax. The HS wax configuration produced melting at a uniform rate and enabled better removal of heat because the internal conductivity of the fins was greater than that of the wax itself. Although PCM systems can provide enhanced operating times up to five times longer under very low heat flux conditions, the maximum latent capacity and liquid-phase thermal resistance due to latent heat are still the overall limiting factors when considering using them in high-flux applications.

The results from this study have significant implications for the design of compact thermal buffers used in aerospace avionics, electric vehicle power modules and 5G telecoms hardware where transient burst loads are typically encountered. Future work should investigate utilizing nano-enhanced PCMs (NePCM) in the sectional designs as a method to further minimize the liquid-phase thermal resistance and, investigate functionally graded (porous) structures or variable thickness air channels to optimize the weight-to-performance trade-off. Experimental validation of the sectional geometries under varying (non-constant) heat flux conditions would also provide additional understanding of the actual performance of hybrid passive-active cooling systems when subjected to real-world conditions.

Declaration of Competing Interest

The authors declare that there are no conflicts of interest regarding the publication of this manuscript.

Funding Information

No funding was received from any financial organization to conduct this research

Author Contributions

All authors proposed the research problem. In addition, Maryam Alathraa Saad: Conceptualization, Methodology, Investigation, Data curation, Writing – original draft. Abbas J. Jubear Al-Jassani: Supervision, Validation, Formal analysis, Writing – review and editing. Mohammed G. Muhssen: Experimental setup, Resources, Data analysis, Visualization. Adel G. Nasser: Project administration, Funding acquisition, Writing – review and editing. All authors have read and agreed to the published version of the manuscript.

Nomenclature

Abbreviations	Meaning
PCM	Phase Change Material
TES	Thermal Energy Storage
TER	Thermal Enhancement Ratio
OM	Organic Material
HS	Hybrid Stearate
LHTES	Latent Heat Thermal Energy Storage
Symbol	Meaning
v	Velocity vector ($m \cdot s^{-1}$)
p	Pressure (Pa)
T	Temperature (K)
Ts	Solidus Temperature (K)
T_1	Liquidus Temperature (K)
f	Liquid fraction
$cp_{,eff}$	Effective specific heat capacity ($J \cdot kg^{-1} \cdot K^{-1}$)
k_{eff}	Effective thermal conductivity ($W \cdot m^{-1} \cdot K^{-1}$)
L_H	Latent heat of fusion ($J \cdot kg^{-1}$)
K	Permeability of porous medium (m^2)
Cf	Forchheimer inertial coefficient
Am	Mushy zone constant ($kg \cdot m^{-3} \cdot s^{-1}$)
α	thermal diffusivity (m2 s-1)
β	Thermal expansion coefficient (K^{-1})
ϕ	Porosity of metal foam
ρ_{eff}	Effective density ($kg \cdot m^{-3}$)
μ	dynamic viscosity (kg m-1s-1)

References

[1] P. J. Shamberger and N. M. Bruno, "Review of Metallic Phase Change Materials for High Heat Flux Transient Thermal Management Applications," *Appl Energy*, vol. 258, no. 113955, 2020, https://doi: 10.1016/j.apenergy.2019.113955.

[2] C. Liu *et al.*, "Phase change materials application in battery thermal management system: A review," Oct. 02, 2020, *MDPI AG*. https://doi: 10.3390/ma13204622.

[3] A. Arshad, M. Jabbal, H. Faraji, P. Talebizadehsardari, M. Anser Bashir, and Y. Yan, "Thermal performance of a phase change material-based heat sink in presence of nanoparticles and metal-foam to enhance cooling performance of electronics," *J Energy Storage*, vol. 48, no. 103882, 2021, https://doi: 10.1016/j.est.2021.103882.

[4] E. M. Ismail, S. J. Flayh, M. Saeedmohammed, and K. S. Mohammed, "Heat Exchanger Design and Optimization for Industrial Applications," *Nanotechnol Percept*, vol. 20, no. S3, pp. 211–229, 2024, https://doi: 10.62441/nano-ntp.v20is3.18.

[5] D. W. Hengeveld, M. R. Wilson, J. A. Moulton, B. S. Taft, and A. M. Kwas, "Thermal design considerations for future high-power small satellites," in *48th International Conference on Environmental Systems*, Albuquerque, New Mexico, Jul. 2018.

[6] M. Saeed Mohammed, S. Fahad Dakel, A. Kadhim Alshara, and A. Mohsin Alsayah, "Numerical and experimental study of heat transfer in shell-and U-tube heat exchanger with baffles," *Chinese Journal of Geotechnical Engineering*, vol. 44, no. 5, pp. 11–26, Jan. 2022, https://doi: 10.11779/CJGE202205.2.

[7] C. Y. Zhao, W. Lu, and Y. Tian, "Heat transfer enhancement for thermal energy storage using metal foams embedded within phase change materials (PCMs)," *Solar Energy*, vol. 84, no. 8, pp. 1402–1412, Aug. 2010, https://doi: 10.1016/j.solener.2010.04.022.

[8] J. Duan and F. Li, "Transient heat transfer analysis of phase change material melting in metal foam by experimental study and artificial neural network," *J Energy Storage*, vol. 33, Jan. 2021, https://doi: 10.1016/j.est.2020.102160.

[9] M. Chen, Y. Wang, and Z. Liu, "Experimental study on micro-encapsulated phase change material slurry flowing in straight and wavy microchannels," *Appl Therm Eng*, vol. 190, May 2021, https://doi: 10.1016/j.applthermaleng.2021.116841.

[10] J. Stever, H. Ma, and T. Supervisor, "Thermal Properties of Disodium Hydrogen Phosphate Dodecahydrate Coated Metal Foam/Sodium Acetate Trihydrate Composite as Phase Change Material," 2022.

[11] A. Mirshekar, M. R. Goodarzi, D. Mohebbi-Kalhori, and M. H. Shafiei Mayam, "Experimental study of heat transfer enhancement using metal foam partially filled with phase change material in a heat sink," *J Energy Storage*, vol. 60, Apr. 2023, https://doi: 10.1016/j.est.2022.106496.

[12] T. Si, W. Cui, T. Ma, L. Lu, and Q. Wang, "Numerical investigation on thermal performance of phase change materials embedded in functionally graded metal foam," *J Energy Storage*, vol. 81, Mar. 2024, https://doi: 10.1016/j.est.2024.110482.

[13] PAN Hanting, Dong Xu, Hongwu Xu, and LUO Zhuqing, "Numerical Analysis on Thermal Performances of Metal Foam Composite Phase Change ," *Yingyong shuxue he lixue (Applied Mathematics and Mechanics)*, vol. Vol. 45, no. Iss: 1, Jan. 2024.

[14] Q. Zhang, M. Wang, Z. Huang, Y. Zhang, and Y. Zhang, "Heat Transfer Improvement of Phase Change Material With Metal Foam," in *2024 Conference of Science and Technology for Integrated Circuits, CSTIC 2024*, Institute of Electrical and Electronics Engineers Inc., 2024. https://doi: 10.1109/CSTIC61820.2024.10531868.

[15] V. Bianco, M. De Rosa, and K. Vafai, "Phase-change materials for thermal management of electronic devices," *Appl Therm Eng*, vol. 214, Sep. 2022, https://doi: 10.1016/j.applthermaleng.2022.118839.

[16] Y. Xu, J. Wang, and T. Li, "Experimental study on the heat transfer performance of a phase change material based pin-fin heat sink for heat dissipation in airborne equipment under hypergravity," *J Energy Storage*, vol. 52, Aug. 2022, https://doi: 10.1016/j.est.2022.104742.

[17] M. Sivashankar and C. Selvam, "Experimental investigation on the thermal performance of low-concentrated photovoltaic module using various pin-fin configurations of heat sink with phase change materials," *J Energy Storage*, vol. 55, Nov. 2022, https://doi: 10.1016/j.est.2022.105575.

[18] V. Safari, B. Kamkari, M. Zandimagham, and N. Hewitt, "Transient thermal behavior of a passive heat sink integrated with phase change material: A numerical simulation," *International Journal of Thermofluids*, vol. 20, Nov. 2023, https://doi: 10.1016/j.ijft.2023.100454.

[19] M. Bouguila, A. Samet, M. A. Ben Souf, A. El Hami, and M. Haddar, "Thermal performances of finned heat sink filled with nano-enhanced phase change materials: Design optimization and parametric study," *Int J Heat Mass Transf*, vol. 202, Mar. 2023, https://doi: 10.1016/j.ijheatmasstransfer.2022.123710.

[20] S. Pourhemmati and S. Hossainpour, "Thermal improvement of the vertical plate-fin heat sink by variable fin thickness pattern and utilizing phase change material: A numerical investigation," *J Energy Storage*, vol. 59, Mar. 2023, https://doi: 10.1016/j.est.2022.106480.

[21] A. H. F. Theeb and I. Y. Hussain, "Numerical simulation of thermal performance of heat sink augmented with phase change material PCM integrated with solid and aluminum metal foam fins," *Heat Transfer*, Nov. 2024, https://doi: 10.1002/htj.23113.

[22] I. Al Siyabi, S. Khanna, T. Mallick, and S. Sundaram, "Multiple Phase Change Material (PCM) Configuration for PCM-Based Heat Sinks-An Experimental Study," *Energies (Basel)*, vol. 11, no. 7, 2018, https://doi: 10.3390/en11071629.

[23] Y. Li, Z. Niu, X. Huang, X. Gao, X. Yang, and B. Sundén, "Effect of pore density and filling ratio of metal foam on melting performance in a heat storage tank," *Numeri Heat Transf A Appl*, 2023, https://doi: 10.1080/10407782.2023.2279290.

[24] A. Nassar *et al.*, "Enhancing the thermal transfer properties of phase change material for thermal energy storage by impregnating hybrid nanoparticles within copper foams," *Results in Engineering*, vol. 21, Mar. 2024, https://doi: 10.1016/j.rineng.2024.101885.

[25] M. Maroliya, V. C. Midhun, and S. K. Saha, "Evaluation of solid-solid and solid-liquid phase change materials in pin-finned heat sinks for cooling of avionics electronics," *Thermal Science and Engineering Progress*, vol. 53, p. 102781, 2024, https://doi.org/10.1016/j.tsep.2024.102781.

[26] L. A. Naeem, T. A. Al-Hattab, and M. I. Abdulwahab, "Study of the Performance of Paraffin Wax as a Phase Change Material in Packed Bed Thermal Energy Storage System," *Iraqi Journal of Chemical and Petroleum Engineering*, vol. 17, no. 4, pp. 25–33, 2016, https://www.iasj.net

[27] A. Veismoradi, A. Modir, M. Ghalambaz, and A. Chamkha, "A phase change/metal foam heatsink for thermal management of battery packs," 2020.

[28] P. Di Giorgio *et al.*, "Numerical Analysis of a Paraffin/Metal Foam Composite for Thermal Storage," in *Journal of Physics: Conference Series*, Institute of Physics Publishing, Mar. 2017. https://doi: 10.1088/1742-6596/796/1/012032.

[29] D. Guarda *et al.*, "Phase Change Material numerical simulation: enthalpy-porosity model validation against liquid fraction data from an X-ray computed tomography measurement/system," *Nondestructive Testing and Evaluation*, vol. 37, no. 5, pp. 508–518, 2022, https://doi: 10.1080/10589759.2022.2070164.

[30] C. Naldi, M. Dongellini, and G. L. Morini, "The evaluation of the effective thermal conductivity of metal-foam loaded phase change materials," *J Energy Storage*, vol. 51, p. 104450, 2022, https://doi: https://doi.org/10.1016/j.est.2022.104450.

[31] A. Rakotondrandisa, G. Sadaka, and I. Danaila, "A finite-element toolbox for the simulation of solid–liquid phase-change systems with natural convection," *Comput Phys Commun*, vol. 253, p. 107188, 2020, https://doi.org/10.1016/j.cpc.2020.107188.